



Kallikrein 7 Promotes Atopic Dermatitis-Associated Itch Independently of Skin Inflammation

Changxiong J. Guo^{1,2,5}, Madison R. Mack^{2,3,5}, Landon K. Oetjen^{2,3}, Anna M. Trier^{2,3}, Martha L. Council³, Ana B. Pavel⁴, Emma Guttman-Yassky⁴, Brian S. Kim^{1,2,3} and Qin Liu^{1,2}

Atopic dermatitis (AD) is a highly prevalent, itchy inflammatory skin disorder that is thought to arise from a combination of skin barrier defect and immune dysregulation. Kallikreins (KLK), a family of serine proteases with a diverse array of homeostatic functions, including skin desquamation and innate immunity, are hypothesized to contribute to AD pathogenesis. However, their precise role in AD has not been clearly defined. In this study, RNA sequencing analyses identified *KLK7* as the most abundant and differentially expressed KLK in both human AD and murine AD-like skin. Further, in mice, *Klk7* expression was localized to the epidermis in both steady state and inflammation. Unexpectedly, *KLK7* was dispensable for the development of AD-associated skin inflammation. Instead, *KLK7* was selectively required for AD-associated chronic itch. Even without the alleviation of skin inflammation, *KLK7*-deficient mice exhibited significantly attenuated scratching, compared with littermate controls, after AD-like disease induction. Collectively, our findings indicate that *KLK7* promotes AD-associated itch independently from skin inflammation and reveal a previously unrecognized epidermal-neural mechanism of AD associated itch.

Journal of Investigative Dermatology (2020) 140, 1244–1252; doi:10.1016/j.jid.2019.10.022

INTRODUCTION

Atopic dermatitis (AD) is a chronic and relapsing inflammatory skin disorder that affects 10–20% of the population (DaVeiga, 2012; Silverberg, 2017). In moderate or severe forms, the crusted, oozing, and itchy skin lesions can dramatically lower the quality of life for patients with AD (Drucker et al., 2017). Although chronic itch (pruritus) is considered the central and most debilitating symptom of AD, treatments have almost exclusively targeted pro-inflammatory mediators, rather than specific pruritogenic pathways.

AD is currently thought to arise from a combination of skin barrier dysfunction and immune dysregulation (Brunner et al., 2018; Czarnowicki et al., 2019; Elias et al., 2008). Many recent studies have focused on how epidermal barrier defects (e.g., filaggrin mutations) lead to the initiation of

allergic inflammation, characterized by the recruitment and activation of T helper type 2 cells, group 2 innate lymphoid cells, and basophils in the affected skin (Esaki et al., 2015; Howell et al., 2007; Kim, 2015; Mashiko et al., 2017; Palmer et al., 2006). These cells, in turn, produce the hallmark type 2 effector cytokines, IL-4, IL-5, and IL-13, which are central to AD immune dysregulation (Brandt and Sivaprasad, 2011; Guttman-Yassky et al., 2019). However, despite our increasing understanding of the inflammatory pathogenesis of AD, the molecular mechanisms of AD-associated itch remain poorly defined.

The kallikrein (KLK) family of serine proteases is hypothesized to be a significant contributor to AD pathology. A number of KLKs are reported to be enriched in the lesional AD skin of humans (Komatsu et al., 2007, 2005; Morizane et al., 2012; Vasilopoulos et al., 2011) and may contribute to AD-associated pruritus in patients (Nattkemper et al., 2018). Moreover, the overexpression of KLKs in murine skin can spontaneously lead to an AD-like disease (Briot et al., 2009; Hansson et al., 2002).

In humans, the KLK family is comprised of 15 structurally conserved members (KLK1–15) that are involved in an array of homeostatic and disease processes across a wide variety of tissues (Shaw and Diamandis, 2007; Sotiropoulou et al., 2009). In healthy human skin, serine peptidase activity in the stratum corneum is mainly attributed to the trypsin-like KLK5 (Deraison et al., 2007; Ekholm et al., 2000) and the chymotrypsin-like KLK7 (Borgoño et al., 2007; Caubet et al., 2004; Yousef et al., 2000), which help maintain barrier homeostasis by regulating the cleavage of corneodesmosomes. Notwithstanding this, a number of other KLKs may also be present in lower abundance and have related functions (Borgoño et al., 2007; Komatsu et al., 2007, 2005, 2003).

¹Department of Anesthesiology, Washington University School of Medicine, St. Louis, Missouri, USA; ²Center for the Study of Itch and Sensory Disorders, Washington University School of Medicine, St. Louis, Missouri, USA; ³Department of Medicine, Division of Dermatology, Washington University School of Medicine, St. Louis, Missouri, USA; and ⁴Department of Dermatology, Icahn School of Medicine at Mount Sinai, New York, New York, USA

⁵These authors contributed equally to this work.

Correspondence: Brian S. Kim, 660 S. Euclid Avenue, Campus Box 8123, Saint Louis, MO 63110.; E-mail: briankim@wustl.edu or Qin Liu, 660 S. Euclid Avenue, Campus Box 5084, Saint Louis, MO 63110. E-mail: qinliu@wustl.edu

Abbreviations: AD, atopic dermatitis; DRG, dorsal root ganglia; KLK, kallikrein; MC903, calcipotriol; PFA, paraformaldehyde; RNA-Seq, RNA sequencing; RT-qPCR, quantitative reverse transcriptase-PCR

Received 10 May 2019; revised 10 October 2019; accepted 31 October 2019; accepted manuscript published online 26 December 2019; corrected proof published online 5 February 2020

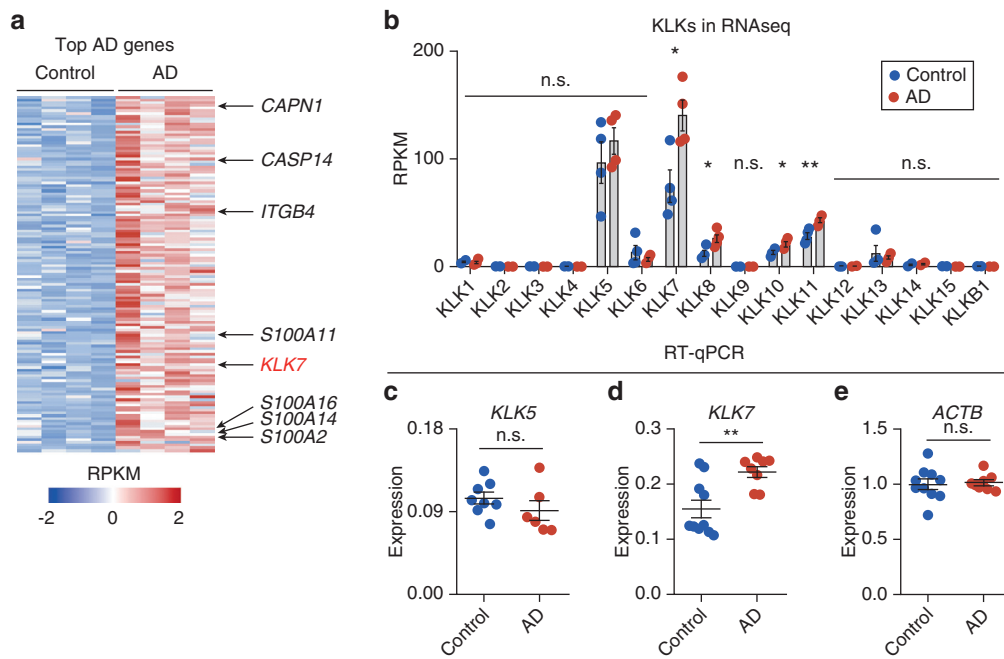


Figure 1. *KLK7* is overexpressed in human lesional AD skin. (a) Heatmap of z-scored RPKMs of differentially expressed genes with >2-fold change, adjusted $P < 0.05$, and base mean expression level > 1,000. (b) RPKMs of all human *KLKs* present in skin samples of control and AD individuals. $N = 4$ per group. (c–e) RT-qPCR of (c) *KLK5* and (d) *KLK7* in human control and AD skin, normalized to (e) *ACTB*. $N = 8–10$ per group. Error bars = standard error of the mean. * $P < 0.05$. ** $P < 0.01$. AD, atopic dermatitis; *KLK*, kallikrein; n.s., no significance; RPKM, reads per kilobase of transcript, per million mapped reads; RT-qPCR, quantitative reverse transcriptase–PCR.

All *KLKs* are translated as pre–pro–enzymes and secreted into the extracellular space as inactive zymogens. There, they are activated by a variety of mechanisms, including autocatalytic activity, endopeptidases, or by other *KLKs* (Sotiropoulou et al., 2009). In the skin, *KLK* activity is further controlled by a number of homeostatic processes, including the endogenous activity of serine protease inhibitors (serpins), such as lymphoepithelial Kazal-type inhibitor encoded by *SPINK5* (Deraison et al., 2007). In the setting of AD, it is hypothesized that the over activity of epidermal *KLKs* set off a cascade of proteolytic activity, which in turn contributes to barrier defects and AD pathogenesis.

In lesional AD skin, a number of *KLKs*, including *KLK5* and *KLK7*, have been shown to be increased (Brunner et al., 2017; Komatsu et al., 2007; Morizane et al., 2012; Vasilopoulos et al., 2011). Furthermore, the transgenic overexpression of *Klk5* or *Klk7* in mice resulted in the spontaneous development of AD-like disease features (Briot et al., 2009; Furio et al., 2014; Hansson et al., 2002). Likewise, loss-of-function mutations in *SPINK5* resulted in unregulated epidermal *KLK* activity and Netherton Syndrome, a severe AD-like syndrome, in both mice and humans (Chavanas et al., 2000; Descargues et al., 2005). In mice, the symptoms of Netherton Syndrome can be prevented by the genetic ablation of *Klk5* and *Klk7* (Kasperek et al., 2017). Although it is becoming increasingly clear that *KLK* dysregulation contributes to AD pathogenesis, the mechanisms underlying this process remain poorly defined.

In this study, we demonstrate that *KLK7*, but not *KLK5*, is upregulated in human and murine lesional AD skin. Further, we show that basal and AD-associated *KLK7* expression is restricted to the epidermis, provoking the hypothesis that epithelial cell-derived *KLK7* is critically required for the development AD. Surprisingly, we found that *KLK7*-deficient mice had no improvement in AD-like skin disease severity but showed markedly attenuated AD-associated itch. These

findings demonstrate a previously unrecognized role for *KLK7* in mediating itch in the context of AD, and provide additional insight into *KLK* function in disease states.

RESULTS

KLK7 is upregulated in human AD lesions

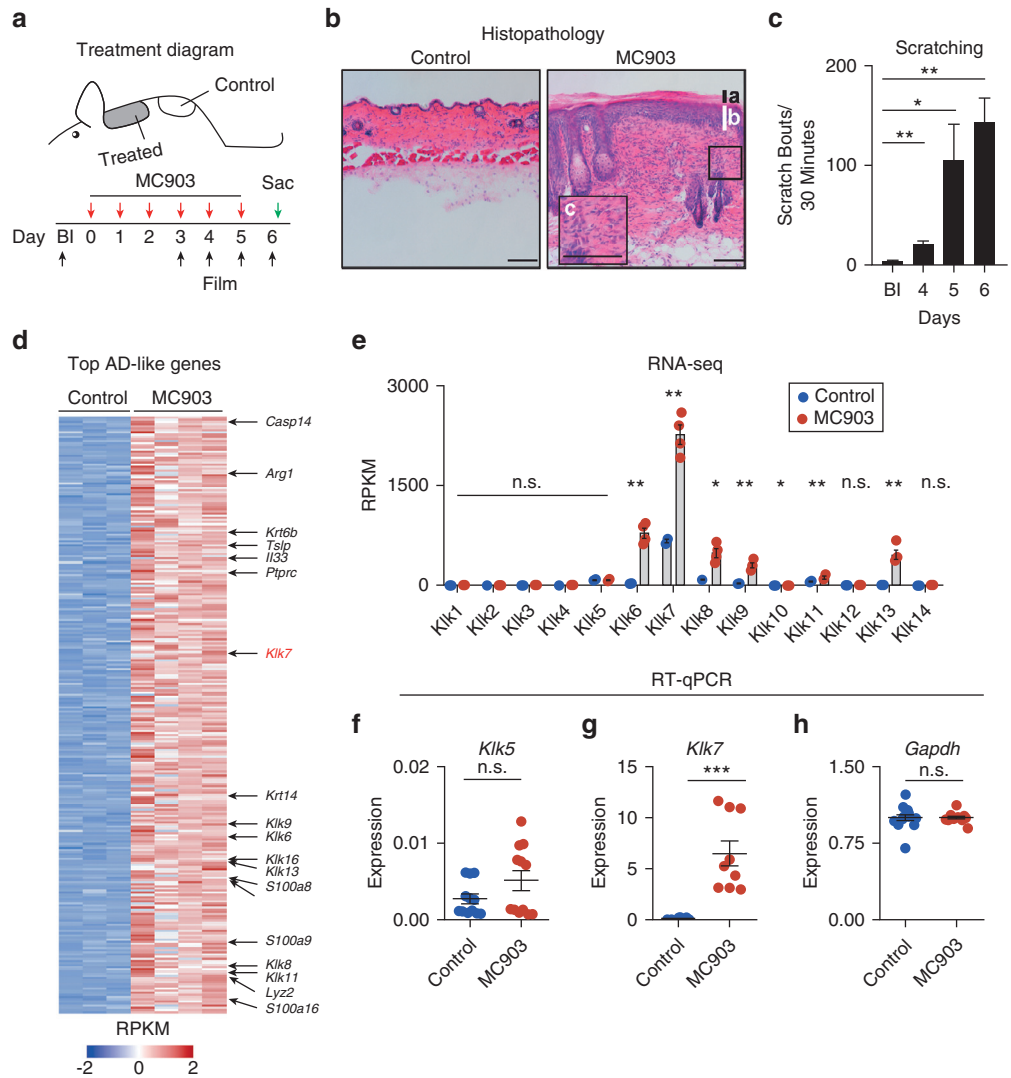
Both human AD and murine AD-like disease are characterized by several shared histological and immunological features. At the molecular level, these include a variety of *KLKs* upregulated in lesional AD skin (Komatsu et al., 2007). However, which *KLKs* are selectively and critically upregulated remains to be defined.

In this study, we reanalyzed a previously published RNA sequencing (RNA-Seq) dataset of human control and lesional AD skin for the top differentially expressed genes by fold change and expression level (Oetjen et al., 2017). Unbiased analysis of the most abundant differentially expressed genes identified *KLK7* as the only *KLK* that was differentially upregulated in human AD skin (Figure 1a). Other keratinocyte-associated genes, such as the *S100A* family members, *CAPN1*, and *CASP14*, were also enriched in AD skin (Figure 1a). Comprehensive analysis of all the *KLKs* in this dataset demonstrated that, consistent with prior studies, *KLK5* and *KLK7* are the most highly expressed *KLKs* in control human skin, accounting for two-thirds of the total *KLK* transcripts in control biopsies (Figure 1b). In addition, four *KLKs*—*KLK7*, *KLK8*, *KLK10*, and *KLK11*—showed statistically significant expression increases in lesional AD skin, with *KLK7* exhibiting the most prominent overexpression. Changes in *KLK8*, *KLK10*, and *KLK11* expression were comparatively less pronounced. Surprisingly, *KLK5* expression was unchanged.

Our finding that *KLK7* is selectively overexpressed in lesional AD skin compared with *KLK5* was further confirmed using additional sets of human control and AD skin samples. Using quantitative reverse transcriptase–PCR (RT-qPCR), we confirmed that *KLK7*, but not *KLK5*, was significantly

Figure 2. *Klk7* is overexpressed in

lesional murine AD-like skin. (a) Schematic of murine AD model. Control skin tissues were taken from nonlesional skin caudal to the treated area. **(b)** Representative hematoxylin & eosin section of control and lesional mouse skin after six MC903 treatments. Note the presence of hyperkeratosis **(a)**, acanthosis **(b)**, and mixed lymphocyte infiltration **(c)** that define human AD lesions. N = 3 biological pairs. **(c)** Mice develop severe spontaneous scratching behavior directed at the treated site after the MC903 treatment. Statistical comparisons are made against baseline scratching. N = 6 mice. **(d, e)** RNA-Seq of mouse control (ethanol vehicle) and MC903-treated skin, N = 3–4 mice per group. **(d)** Heatmap showing z-scored RPKMs of genes differentially expressed by \geq two-fold, adjusted $P < 0.05$, and base mean expression values $\geq 1,000$. **(e)** RPKM values of all the *Klks* expressed in skin samples of control- and MC903-treated mice. **(f–h)** RT-qPCR of **(f)** *Klk5* and **(g)** *Klk7* expression in mouse control- and MC903-treated skin normalized to **(h)** *Gapdh*. N = 3 biological pairs. Error bars = standard error of the mean. * $P < 0.05$. ** $P < 0.01$. *** $P < 0.001$. Bars = 200 μ m. AD, atopic dermatitis; MC903, calcipotriol; n.s., no significance; RPKM, reads per kilobase of transcript, per million mapped reads; RT-qPCR, quantitative reverse transcriptase-PCR;



enriched in lesional AD skin (Figure 1c–e). Additionally, we looked specifically at matched lesional and nonlesional sites in another cohort of 35 patients with AD by RNA-Seq (Supplementary Figure S1a and b). Consistent with the observations from our other cohorts, we found no increases in *KLK5* expression in lesional AD skin in this dataset (Supplementary Figure S1a). Moreover, we confirmed that *KLK7* mRNA is significantly elevated in lesional AD skin, compared with matched nonlesional sites (Supplementary Figure S1b). However, the variations in *KLK7* levels within lesional tissues did not significantly correlate with patient-reported itch severity (Supplementary Figure S1c). Based on these results, we hypothesized that *KLK7* may be a key driver in AD disease pathogenesis.

***Klk7* is upregulated in murine AD-like lesions**

Since KLKs are highly conserved across mammalian species (Pavlopoulou et al., 2010), we explored whether *Klk7* expression is also dysregulated in murine AD-like skin. To test this, we employed a well-established model of AD-like disease, in which mice are treated with the topical irritant MC903 (calcipotriol) (Li et al., 2006) (Figure 2a). Following

MC903 treatment, mice develop the histopathologic features of AD (Figure 2b), as well as chronic itch behavior (Figure 2c).

To define the expression status of *Klk7* in mouse AD-like skin, we reanalyzed a previously published RNA-Seq dataset of MC903-treated murine AD-like skin (Oetjen et al., 2017). Using the same unbiased analysis technique, we identified *Klk7* among the top most abundant differentially expressed genes in murine AD-like skin (Figure 2d). A comprehensive analysis of all the *Klks* in this dataset demonstrated that, like human skin (Figure 1), *Klk7* was the most highly expressed *Klk* in control skin, accounting for $66.9\% \pm 1.43\%$ of the total *Klk* transcripts. Moreover, seven *Klks* – *Klk6*, *Klk7*, *Klk8*, *Klk9*, *Klk10*, *Klk11*, and *Klk13* – showed statistically significant increases in expression in murine AD-like skin (Figure 2e). Similar to our findings in human AD skin, *Klk7* was the most abundant transcript and demonstrated a four-fold increase in expression in AD-like skin (Figure 2e). *Klk5* expression, again, was unchanged in this context (Figure 2e). These findings were further validated with additional samples by RT-qPCR. *Klk7*, but not *Klk5*, was significantly enriched in AD-like skin (Figure 2f–h).

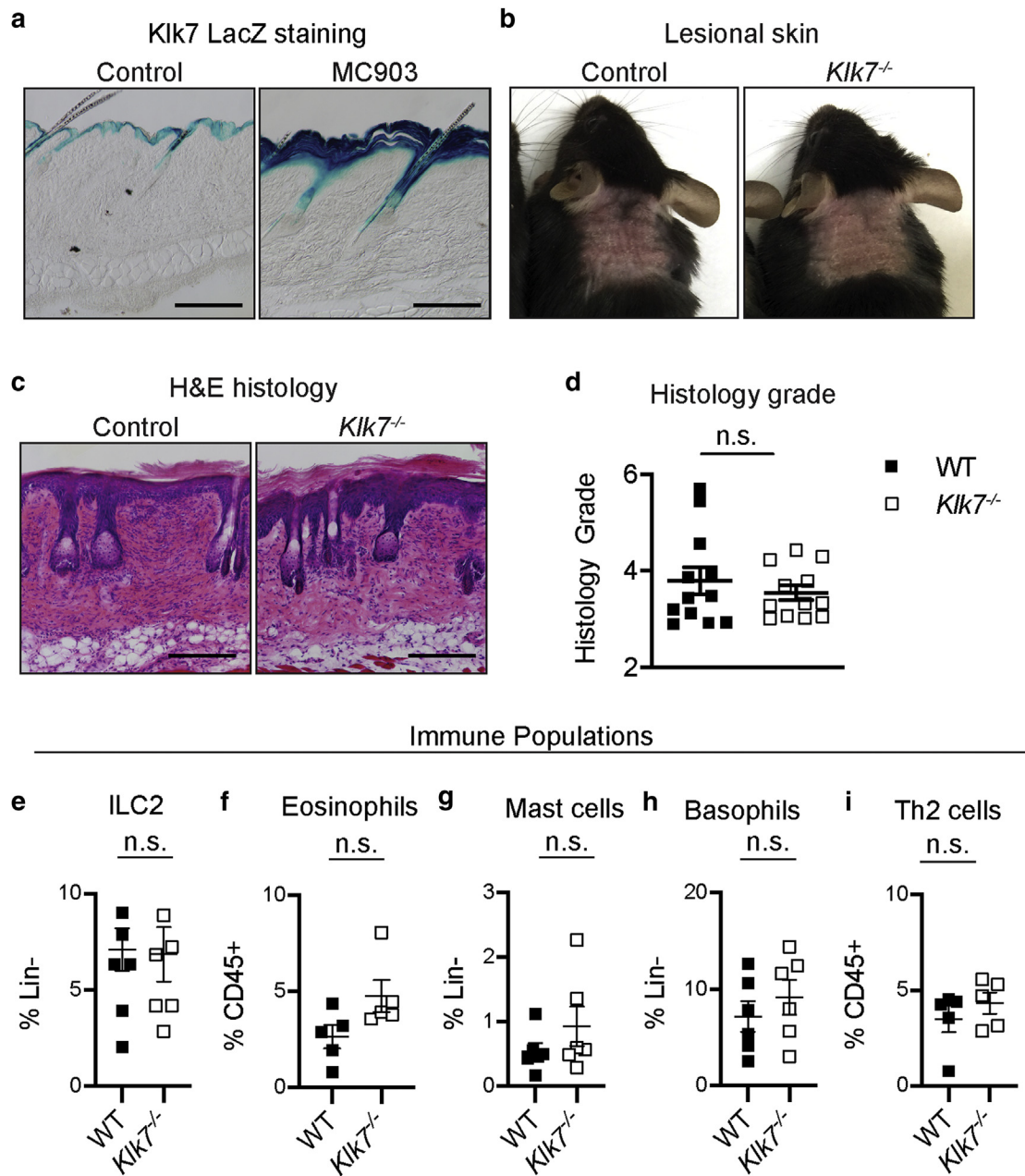


Figure 3. *Klk7* deficiency does not cause defects in AD-associated immune response. (a) X-gal staining of nape skin from *Klk7*^{LacZ} mice without treatment (control) and after treatment with MC903. (b) Representative images of AD-like disease induction in control (wild-type) and *Klk7*^{-/-} mice after 6 days of MC903 treatment; N ≥ 8 mice per group. (c) Representative H&E-stained sections of MC903-treated skin of control and *Klk7*^{-/-} mice; N = 4 mice per group. (d) Histological grading of H&E-stained sections of control and *Klk7*^{-/-} mouse skin; N = 4 mice per group. (e–i) Flow cytometric analysis of AD-associated (e) ILC2, (f) eosinophil, (g) mast cell, (h) basophil, and (i) Th2 cell frequency in MC903-treated nape skin from control and *Klk7*^{-/-} mice on day 6 of treatment; n = 5 mice per group. Error bars = standard error of the mean. Scale bars = 200 μm. AD, atopic dermatitis; H&E, hematoxylin and eosin; ILC2, group 2 innate lymphoid cell; n.s., no significance; Th2, T helper type 2; WT, wild-type; X-gal, 5-bromo-4-chloro-3-indolyl-β-D-galactopyranoside.

Based on the consistent *KLK7* upregulation in AD skin of both humans and mice, we sought to investigate the mechanisms by which *KLK7* promotes AD-like disease pathogenesis *in vivo*.

Epidermal *Klk7* expression is enhanced in AD-like disease and promotes itch but not inflammation

Klk7 expression is highly conserved between mice and humans and is mainly restricted to the skin in both species (Fagerberg et al., 2014; Pavlopoulou et al., 2010). In the steady state, murine *Klk7* expression is largely restricted to

epidermal skin and is undetectable in dermal skin, neural, and immune tissues (Figure 3a and Supplementary Figure S2). After the induction of AD-like disease, *Klk7*, detected using a *LacZ*-β-galactosidase reporter, was selectively enhanced in the epidermis, but remained undetectable in the dermis where infiltrating immune cells and peripheral fibers of sensory neurons are present (Figure 3a). Taken together, these findings indicate that the epidermis is the primary source of *Klk7* in the skin, in both homeostatic and inflammatory conditions.

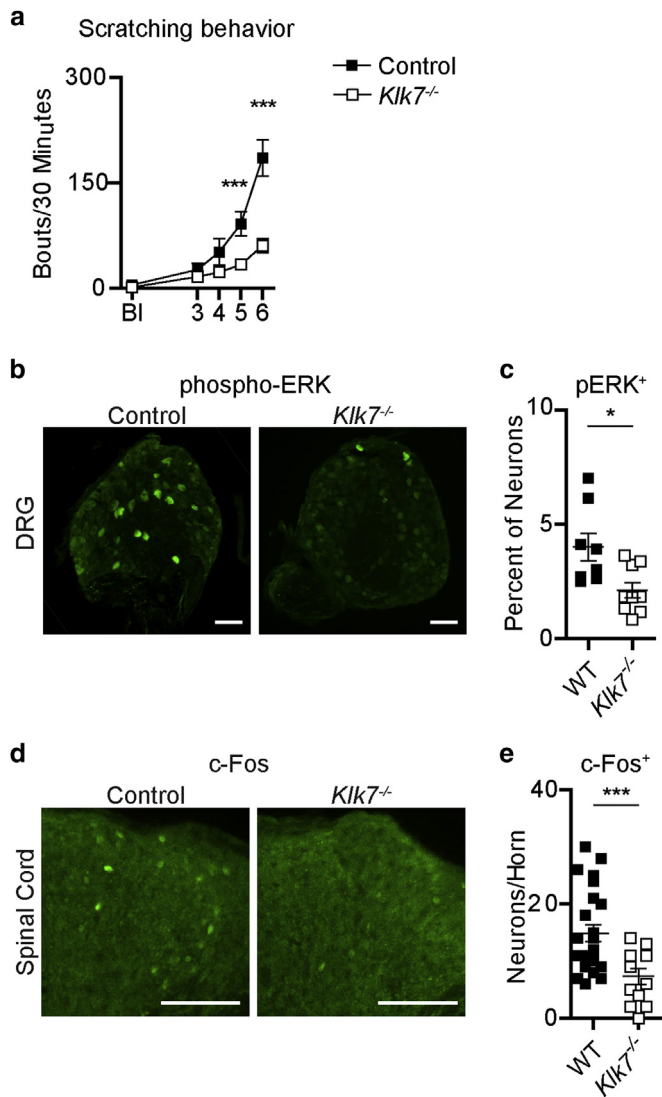


Figure 4. *Klf7* is required for the development of AD-associated itch. (a) Spontaneous scratching after MC903 nape treatment in control and *Klf7*^{-/-} mice; N > 8 per group. (b, c) (b) Representative immunofluorescent images and (c) quantification of phosphorylated ERK staining in DRG innervating MC903-treated nape skin of control and *Klf7*^{-/-} mice; N = 3 mice per group. (d, e) (d) Representative immunofluorescent images and (e) quantification of c-Fos staining in thoracic spinal cords of MC903-treated control and *Klf7*^{-/-} mice on day 6 of treatment; N = 3 mice per group. Error bars = standard error of the mean. **P* < 0.05. ****P* < 0.001. Scale bars = 200 μm. BI, baseline; DRG, dorsal root ganglia; ERK, mitogen-activated protein kinase 3/1; MC903, calcipotriol; WT, wild-type.

To directly investigate the contribution of KLK7 to AD-like skin disease, we generated the MC903-induced AD-like disease model using *Klf7*^{-/-} mice. Surprisingly, compared with the wild-type controls, *Klf7*^{-/-} mice did not exhibit a significant reduction in disease severity as measured by redness, edema or papulation, scaling, and lichenification (enhanced skin lines) (Figure 3b). Additionally, histological analyses did not demonstrate any difference between groups by clinical grading (Figure 3c–d). A flow cytometric analysis of the skin from control and *Klf7*^{-/-} mice also did not reveal any difference in the frequency of key inflammatory cells (Figure 3e–i).

Additional quantification of T helper type 2 cells and inflammatory markers did not reveal any detectable differences between MC903-treated control and *Klf7*^{-/-} mice. Serum IgE and TARC/CCL17 levels, as detected by ELISA, were similar between the genotypes (Supplementary Figure S3a–b). The *Il4ra*, *Il4*, and *Il13* expression levels in MC903-treated lesional skin, as detected by RT-qPCR, were also not different between the control and *Klf7*^{-/-} mice (Supplementary Figure S3c–e). Lastly, *Tslp* expression in the skin was strongly induced by MC903 treatment as expected, but was expressed at similar levels between the genotypes at both basal and diseased states (Supplementary Figure S3f).

Despite the lack of observable differences in skin inflammation and key inflammatory markers, spontaneous scratching was markedly reduced in *Klf7*^{-/-} mice, when compared with controls (Figure 4a). On average, *Klf7*^{-/-} mice scratched two to three times less than the controls and demonstrated a mean of 61.33 ± 10.24 bouts per 30 minutes, versus 186.13 ± 25.89 bouts per 30 minutes for the control mice on day 6 of treatment (Figure 4a). These findings were recapitulated in a 12-day ear treatment model, in which *Klf7*^{-/-} mice exhibited a similar reduction in itch (Supplementary Figure S4).

Given the striking itch phenotype, we examined whether sensory neuron activation was correspondingly attenuated in *Klf7*^{-/-} mice under AD-like conditions. Although rarely detectible in primary afferents at baseline, mitogen-activated protein kinase 3/1 phosphorylation can be transiently induced in dorsal root ganglia (DRG) neurons by intense stimulation or under chronic pathological conditions (Gao and Ji, 2009). Upper thoracic DRGs that innervate the inflamed skin showed a substantially diminished proportion of phosphorylated mitogen-activated protein kinase 3/1 immunoreactive neurons in *Klf7*^{-/-} mice, compared with the control mice (2.11 ± 0.34% vs 4.00 ± 0.60%, respectively) (Figure 4b–c), indicating that the activation and sensitization of peripheral sensory neurons were significantly attenuated in *Klf7*^{-/-} mice. Likewise, c-Fos expression, which is induced by the strong and sustained activation of spinal dorsal horn neurons (Gao and Ji, 2009), was significantly decreased in the thoracic spinal cords of *Klf7*^{-/-} mice, most notably in lamina I and II where itch-sensing c-fiber DRG neurons project (Han et al., 2013) (Figure 4d–e). These findings indicate that, along with a reduction in behavioral itch (Figure 4a), sensory neuron activation is significantly attenuated in *Klf7*^{-/-} mice in the context of AD. Collectively, our findings demonstrate that the epidermis is the major source of *Klf7* and reveal a previously unrecognized epithelial-neural circuit by which *Klf7* specifically mediates AD-associated itch.

DISCUSSION

KLKs are highly conserved across species, widely expressed throughout many organ systems, and exhibit heterogeneity in their composition across tissues (Pavlopoulou et al., 2010; Sotiropoulou et al., 2009). As serine proteases, they are involved in a diversity of both homeostatic and pathologic processes. In the skin, their primary role is to

mediate desquamation (Ekholm et al., 2000). Both KLK5 and KLK7 have been shown to be key mediators of corneodesmosomal cleavage and epithelial turnover (Caubet et al., 2004). While a number of KLKs, including KLK5 and KLK7, have been shown to be upregulated in lesional AD skin from patients (Brunner et al., 2018; Komatsu et al., 2007; Morizane et al., 2012; Vasilopoulos et al., 2011), their precise role in AD pathogenesis remains unclear. In this study, we provide three conceptual advances that clarify the contributions of KLKs to AD. First, using an unbiased RNA-Seq analysis, we discovered that *KLK7* is selectively upregulated in the lesional AD skin of both mice and humans. Second, we show that, despite its abundant expression in the skin, *Klk7* is dispensable for the development of AD-associated inflammation. Third, the epidermal expression of *Klk7* is selectively required for AD-associated itch. Importantly, these findings demonstrate an emerging paradigm in itch biology, that itch mediators may be separate from the mechanism driving AD-like skin inflammation.

The induction of the type 2 cytokines IL-4 and IL-13 critically promote AD-associated skin inflammation and itch (Oetjen and Kim, 2018; Trier and Kim, 2018). Additionally, clinical trials with dupilumab, an anti-IL-4R α monoclonal antibody, have demonstrated rapid and marked improvement of itch symptoms in patients with AD (Beck et al., 2014; Guttman-Yassky et al., 2019; Simpson et al., 2016; Thaçi et al., 2016). Recent studies have shown that both IL-4 and IL-13 induce selective expression of KLK7 but not KLK5 in normal human epidermal keratinocyte cells (Morizane et al., 2012). Thus, whether there is a type 2 cytokine-epithelial-KLK circuit promoting itch remains a promising area of future inquiry.

Although prior studies have reported the broad upregulation of a number of KLKs in AD skin (Komatsu et al., 2007; Vasilopoulos et al., 2011), our gene expression analysis only identified *KLK7* as the predominant KLK in both mouse and human AD skin. Despite previous reports that KLK5 is upregulated in human AD skin (Komatsu et al., 2007) and implicated in the promotion of AD-like disease in mice (Briot et al., 2009; Furio et al., 2014), we consistently could not detect *KLK5* upregulation in AD skin. This may be in part due to the complexity of AD disease, with varying stages (acute vs chronic), levels of severity, and genetic- and age-dependent heterogeneity. For example, mutations in filaggrin vary considerably across ethnicities, and there is emerging evidence that immune profiles in AD are also sensitive to the genetic background of individuals (Czarnowicki et al., 2019; Kaufman et al., 2018; Leung, 2015; Margolis et al., 2014; Osawa et al., 2011). Future studies focused on understanding the differential contributions of KLK5 and KLK7 to skin inflammation and itch are therefore warranted. Additionally, it is widely appreciated that KLKs can activate one another (Sotiropoulou et al., 2009). Thus, understanding how KLK7 may interact with other KLKs to regulate the development of AD-associated itch is an intriguing area of investigation.

Prior studies have shown that the overexpression of *Klk7* was particularly notable for the development of severe itch associated with cutaneous inflammation (Hansson et al.,

2002). Despite these advances, whether KLK-mediated itch occurs indirectly through the induction of skin inflammation or directly by acting on sensory neurons was unknown. Our finding that *Klk7* deficiency attenuates AD-associated itch with no effect on inflammation provokes the hypothesis that this phenomenon occurs through direct epidermal-neuronal mechanisms. It has previously been shown that KLK5 can proteolytically activate PAR2 receptors, which have been heavily implicated in itch (Liu et al., 2011; Shimada et al., 2006; Stefansson et al., 2008). However, KLK7 does not exhibit this function (Supplementary Figure S5) (Stefansson et al., 2008) or the ability to induce significant behavioral response or neuronal activation in naïve mice (Supplementary Figure S6a–c). Thus, whether KLK7 generates endogenous pruritogens or if KLK7 can proteolytically sensitize neuronal itch receptors in AD skin remains open to further exploration.

In conclusion, therapeutic agents targeting KLK7 may be able to provide substantial itch relief for patients with AD. Owing to the specificity of KLK7 expression in epidermal skin, KLK7 antagonists could be used topically on affected AD skin to avoid potential side effects. Moreover, given the unique chymotrypsin-like functionality of KLK7, in contrast to the trypsin-like properties of other KLKs, redundancy and compensation by other KLKs is also less likely following pharmacologic KLK7 inhibition. These findings open exciting avenues for the exploration and development of novel therapeutics that target KLKs in the setting of AD and its associated itch.

MATERIALS AND METHODS

Animals

C57BL/6NJ wild-type mice were purchased from The Jackson Laboratory (Bar Harbor, ME). *Klk7^{tm1(KOMP)Vlg}* sperm was purchased from the UC Davis KOMP repository (Davis, CA). IVF was performed by the Washington University School of Medicine Molecular Genetics Service Core. *Pirt^{CCaMP3/+}* mice were a gift from Dr. Xinzhong Dong at Johns Hopkins University. All researchers were blinded to mouse genotypes throughout testing and data quantification.

Human sample collection

AD diagnosis was made by a board-certified dermatologist using the American Academy of Dermatology recommended criteria (Eichenfield et al., 2014). Biopsy samples were collected from consenting patients in clinics. Control tissues were either obtained from individuals without a history of inflammatory skin conditions or from healthy skin margins from patients undergoing Mohs surgery. All the skin samples were de-identified and stored in RNAlater (ThermoFisher, Waltham, MA) at -80°C before processing.

Mouse Tissue Collection

For reverse transcriptase–PCR and RT–qPCR, the mice were euthanized via carbon dioxide overdose, and tissues were dissected and stored in ice cold RNeasy Kit Lysis Buffer (Qiagen, Hilden, Germany). Samples were processed for RNA extraction immediately after dissection.

For histopathology and LacZ staining, the mice were transcardially perfused with ice cold phosphate buffered saline and 4% paraformaldehyde (PFA) for fixation. Dissected tissues were fixed on ice as follows: skin in 1% PFA for 1 hour, DRG and trigeminal ganglia in 2% PFA for 30 minutes, spinal cord in 2% PFA for 1 hour,

and brain in 2% PFA for 2 hours. After fixation, the tissues were immersed in 30% sucrose for 24 hours at 4°C and embedded in O.C.T. (Sakura, Torrance, CA) for frozen sectioning. Mouse DRGs and spinal cords used for immunostaining were fixed in 4% PFA on ice for 90 minutes before sucrose incubation and frozen sectioning. For flow cytometry, the skin was harvested without fixation and processed immediately.

For ELISA, mouse serum was isolated from blood collected by orbital bleed by centrifugation at 10,000g for 10 minutes at 4°C on experimental day 6. ELISAs for IgE (Biolegend 432404, San Diego, CA) and TARC/CCL17 (R&D DY529-05, Minneapolis, MN) were performed according to the manufacturers' instructions.

Hematoxylin and eosin, X-Gal, and immunofluorescence staining

O.C.T.-embedded mouse samples were sectioned on a Leica (Buffalo Grove, IL) cryostat. Brain sections were processed as floating sections, whereas other tissues were slide-mounted. Hematoxylin and eosin staining was performed by the Washington University School of Medicine Pulmonary Morphology Core. Images were acquired using a BX63 microscope (Olympus, Waltham, MA). The clinical grade was determined using a previously published protocol (Kim et al., 2014).

The tissues used for LacZ and immunofluorescence staining were allowed to air dry for 2 hours before processing. For LacZ staining, the slides were fixed on ice in 1% PFA for 1 minute. Chromogenesis was performed using the X-Gal Staining Assay Kit (Genlantis, San Diego, CA) according to the manufacturer's instructions. The color development time was approximately 6 minutes. Sections were dehydrated and mounted using ThermoFisher Permount.

For phosphorylated mitogen-activated protein kinase 3/1 and c-FOS immunofluorescence staining, the slides were blocked using 10% normal goat serum (MilliporeSigma, Burlington, MA) and incubated in primary antibodies overnight at 4°C. Afterwards, the slides were incubated in fluorescent secondary antibody for 2 hours at room temperature and mounted using Fluoromount-G (SouthernBiotech, Birmingham, AL). Images were acquired using a Ti-E microscope (Nikon, Melville, NY). The antibodies used were rabbit anti-phospho-p44/42 mitogen-activated protein kinase (Thr202/Tyr204) monoclonal antibody (CST, Danvers, MA), rabbit anti-c-Fos polyclonal antibody (Calbiochem, San Diego, CA), goat anti-Rabbit IgG (H+L), and Alexa Fluor 488 conjugated secondary (ThermoFisher, Waltham, MA). All the antibodies were diluted 1:1,000 in phosphate buffered saline with 1% Tween-20 and 1% normal goat serum.

RNA isolation, reverse transcriptase-PCR, and RT-qPCR

RNA-Seq was performed and analyzed as previously described (Oetjen et al., 2017). Briefly, for RNA-Seq, 1 µg of total RNA was enriched with RiboZERO (Illumina, San Diego, CA) and sequenced on an Illumina HiSeq3000. Sequences were aligned with STAR (Dobin et al., 2013), counted with Subread:featureCount (Liao et al., 2014), and differential gene expression was determined by the DESeq2 package (Love et al., 2014) in R version 3.5.

The samples for reverse transcriptase-PCR and RT-qPCR were homogenized in lysis buffer supplied with the Qiagen RNeasy Kit using a bead homogenizer. RNA extraction was performed using the same kit, according to the manufacturer's instructions. Samples were then treated with ThermoFisher Turbo DNase, and cDNA was generated using approximately 1,000 ng of total RNA and an ABI

High-Capacity cDNA Reverse Transcription Kit (ABI, Waltham, MA). Reactions without reverse transcriptase were included as negative controls for downstream PCR.

Reverse transcriptase-PCR was performed using Qiagen HotStarTaq Polymerase and 10 ng of template. The images presented are representative of the results of 30 PCR cycles. RT-qPCR was performed using ABI Fast Sybr Green Master Mix and a Step-One Plus Real-Time PCR System. All reactions were run as technical triplicates using 10 ng of cDNA template, and the presented data were normalized to *ACTB* (for human samples) or *Gapdh* (for mouse samples) expression. The primers used are listed in Supplementary Table S1.

MC903 treatment and mouse behavior

The murine AD model was adapted from previous publications (Kim et al., 2014, 2013; Li et al., 2006; Oetjen et al., 2017). In the nape model, the nape and lower back areas (approximately 17 mm × 17 mm each) were shaved under isoflurane anesthesia 3 days before baseline behavioral recording. Test animals were habituated for two consecutive days immediately preceding baseline recording. To induce AD-like disease, 40 µl of 0.1 mM MC903 in ethanol was applied topically to the shaved nape skin under anesthesia once every 24 hours, starting 24 hours after baseline recording, for six consecutive days. Spontaneous scratching was scored for four consecutive days, starting 4 days after the baseline recording. Scratching bouts, defined as a continuous scratch movement directed at the treated skin by the hind paw, were scored from video recordings after the completion of the experiment. For the ear model, mice were treated with 40 µl of 0.05 mM MC903 on each ear under anesthesia for 8 days. The ear thickness was determined daily with a dial caliper.

Flow cytometry

Flow cytometry was performed as previously described (Oetjen et al., 2017). Briefly, harvested tissues were digested in 0.25 mg/ml Liberase TL (Roche, Switzerland) in DMEM media for 90 minutes at 37°C. Afterwards, the tissues were mechanically dissociated and passed through 70 µm cell strainers to obtain a single cell suspension. The cells were then stained with ZombieUV (Biolegend) at room temperature for 20 minutes, followed by primary antibodies (Supplementary Table S2) on ice for 30 minutes. Biolegend streptavidin-FITC and streptavidin-PE secondary stains were performed on ice for 30 minutes. Samples were acquired on an LSRFortessa X-20 (BD, Franklin Lakes, NJ).

Calcium imaging

Calcium imaging was performed as previously described (Huang et al., 2018; Oetjen et al., 2017). In brief, KNRK cells stably expressing hPAR2 receptors (KNRK-PAR2) were seeded onto coverslips precoated with 0.1 mg/ml poly-D-lysine (Corning, Corning, NY) and cultured overnight in DMEM complete medium. Primary cultures of DRG neurons from *Pirt^{Cre}CaMP3^{+/+}* mice were acutely extracted and dissociated in dispase II and collagenase I enzyme mixture from ThermoFisher. Dissociated DRG neurons were then seeded onto coverslips precoated with poly-D-lysine and 0.01 mg/ml laminin (Corning) and cultured overnight in DH10 media supplemented with 25 pg/ml NGF (Corning) and 50 pg/ml GDNF (R&D Systems).

Approximately 24 hours after seeding, KNRK cells were loaded with Fura2-AM (Fisher) and imaged at 340 and 380 nm excitation. DRG neurons were imaged at 488 nm excitation. Images were

acquired using a Nikon (Melville, NY) Ti-E microscope with a Photometrics (Tucson, AZ) HQ2 camera. rhKLK7 (R&D Systems) and trypsin (ThermoFisher) were bath applied. Ratios of 340/380 nm and quantified green fluorescent protein fluorescence were determined using Nikon NIS AR software.

Data analysis

All data are presented as the mean \pm standard error of the mean. Statistical significance for the two groups was determined using a two-tailed, unpaired Student's *t* test. The differences between three or more groups were tested using a one-way analysis of variance, followed by two-tailed Student's *t* tests. Differences were considered significant if $P < 0.05$. Flow cytometry data was analyzed with Treestar (Ashland, OR) Flowjo v10. Graphs were generated using Graphpad (San Diego, CA) Prism 8 and R version 3.5 (Vienna, Austria).

ETHICS STATEMENT

All the animal experiments were performed under protocols approved by the Institutional Animal Care and Use Committee at Washington University School of Medicine and in strict accordance with recommendations in the Guide for the Care and Use of Laboratory Animals of the National Institutes of Health. Human studies were performed under protocols reviewed and approved by local Institutional Review Boards, and biopsies were taken only after obtaining written, informed patient consent.

Data availability statement

Datasets related to this article can be found at the GEO DataSets using accession numbers GSE90883 and GSE140380, hosted at www.ncbi.nlm.nih.gov.

ORCIDiS

Changxiong J Guo: <https://orcid.org/0000-0002-2886-8536>
 Madison R Mack: <https://orcid.org/0000-0003-2812-0349>
 Landon K Oetjen: <https://orcid.org/0000-0001-9985-7837>
 Martha L Council: <https://orcid.org/0000-0002-2657-9060>
 Ana B Pavel: <https://orcid.org/0000-0002-8155-8553>
 Emma Guttman-Yassky: <https://orcid.org/0000-0002-9363-324X>
 Brian S Kim: <https://orcid.org/0000-0002-8100-7161>
 Qin Liu: <https://orcid.org/0000-0003-4333-4951>

CONFLICT OF INTEREST

BSK has consulted for AbbVie, Inc., Concert Pharmaceuticals, Incyte Corporation, Menlo Therapeutics, and Pfizer, Inc. and has been an advisory board participant for Celgene Corporation, Kiniksa Pharmaceuticals, Menlo Therapeutics, Regeneron Pharmaceuticals, Inc., Sanofi, and Theravance Biopharma. BSK is a stockholder of Gilead Sciences, Inc. and Mallinckrodt Pharmaceuticals and founder and Chief Scientific Officer of Nuogen Pharma, Inc. EG has received grants (paid to Mount Sinai Health System), consulting fees, and/or honoraria from AbbVie, Allergan, Anacor, Asana Bioscience, Bristol-Myers Squibb, Celgene Corporation, Celsus Therapeutics, Curadim Pharma, Dermira, Drais, Eli Lilly, Escalier, Galderma, Genentech, Glenmark, Janssen Biotech, Kymab Limited, Kyowa Kirin, Lead Pharma, LEO Pharma, Merck Pharmaceuticals, Novartis, Pfizer, Regeneron, Sanofi, Sienna Biopharmaceuticals, Stiefel/GlaxoSmithKline, Theravance, and Vitae. MLC has consulted for MDO Outlook. MRM, LKO, AMT, CJG, ABP, and QL state no conflict of interest.

ACKNOWLEDGMENTS

Research in the Kim Lab is supported by the Doris Duke Charitable Foundation, Celgene Corporation, LEO Pharma, and the National Institute of Arthritis Musculoskeletal and Skin Diseases of the National Institutes of Health (NIH) [NIH (K08AR065577 and R01AR070116)]. MRM was supported by the NIH National Institute of Allergy and Infectious Diseases T32T32AI00716340. AMT is supported by the NIH National Heart, Lung, and Blood Institute T32 HL007317. The Kim Lab has also been generously supported by donations from Anabeth and John Weil and Carole Kroeger. Research in the Liu Lab is supported by the NIH (R01AI125743), Brain Research Foundation Fay / Frank Seed Grant, and Pew Scholar Award to QL.

The *KLK7^{tm1(KOMP)Vlcg}* mouse strain used for this research project was generated by the trans-NIH Knock-Out Mouse Project and obtained from the Knock-Out Mouse Project Repository (www.komp.org). NIH grants to Velocigena at Regeneron Inc (U01HG004085) and the CSD Consortium (U01HG004080) funded the generation of gene-targeted embryonic stem cells for 8,500 genes, including *KLK7*, in the Knock-Out Mouse Project Program and archived and distributed by the Knock-Out Mouse Project Repository at UC Davis and CHORI (U42RR024244).

AUTHOR CONTRIBUTIONS

Conceptualization: CJG, MRM, QL, BSK; Data curation: MRM; Formal Analysis: CJG, MRM, ABP; Funding Acquisition: QL, BSK, EG; Investigation: CJG, MRM, ABP, LKO, AMT; Methodology: CJG, MRM, QL, BSK; Resources: MRM, BSK, MLC, EG; Supervision: QL and BSK; Validation: MRM, BSK, ABP, EG; Visualization: CJG and MRM; Writing – Original Draft: CJG, MRM, QL, BSK; Writing – Review & Editing: CJG, MRM, AMT, QL, BSK, ABP, and EG.

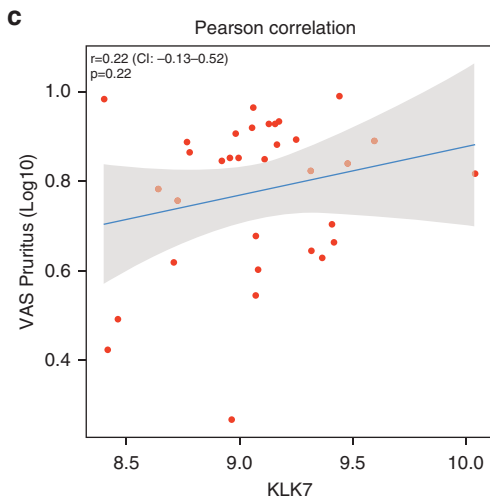
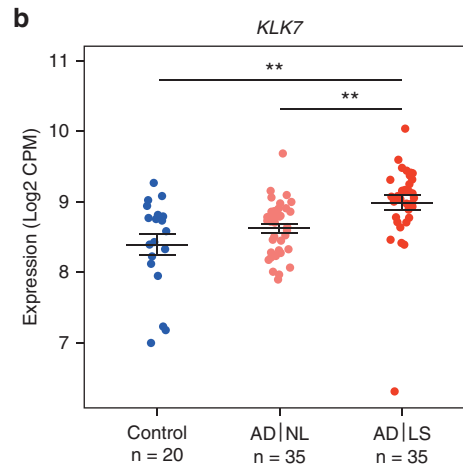
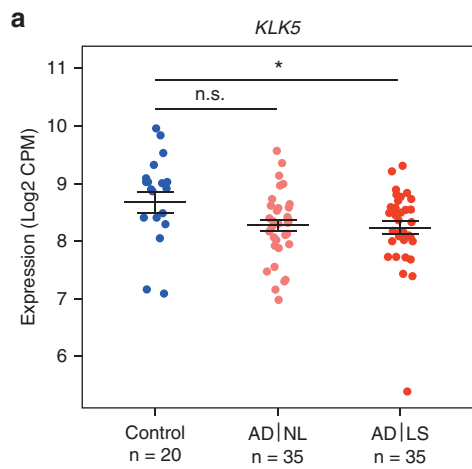
SUPPLEMENTARY MATERIAL

Supplementary material is linked to the online version of the paper at www.jidonline.org, and at <https://doi.org/10.1016/j.jid.2019.10.022>.

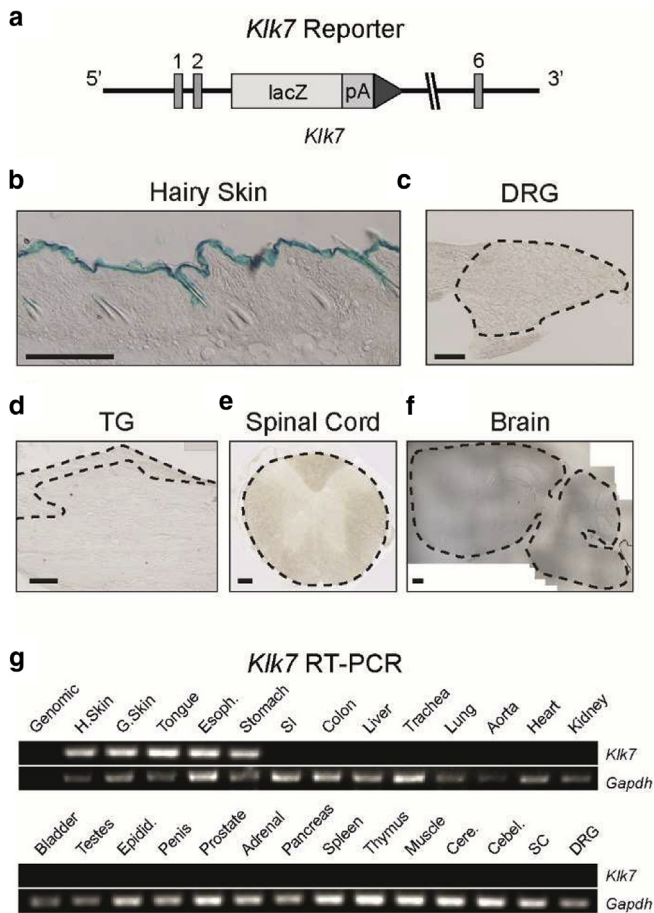
REFERENCES

- Beck LA, Thaçi D, Hamilton JD, Graham NM, Bieber T, Rocklin R, et al. Dupilumab treatment in adults with moderate-to-severe atopic dermatitis. *N Engl J Med* 2014;371:130–9.
- Borgoño CA, Michael IP, Komatsu N, Jayakumar A, Kapadia R, Clayman GL, et al. A potential role for multiple tissue kallikrein serine proteases in epidermal desquamation. *J Biol Chem* 2007;282:3640–52.
- Brandt EB, Sivaprasad U. Th2 cytokines and atopic dermatitis. *J Clin Cell Immunol* 2011;2:1–13.
- Briot A, Deraison C, Lacroix M, Bonnart C, Robin A, Besson C, et al. Kallikrein 5 induces atopic dermatitis–like lesions through PAR2-mediated thymic stromal lymphopoietin expression in netherton syndrome. *J Exp Med* 2009;206:1135–47.
- Brunner PM, Guttman-Yassky E, Leung DYM. The immunology of atopic dermatitis and its reversibility with broad-spectrum and targeted therapies. *J Allergy Clin Immunol* 2017;139:S65–76.
- Brunner PM, Israel A, Zhang N, Leonard A, Wen HC, Huynh T, et al. Early-onset pediatric atopic dermatitis is characterized by TH2/TH17/TH22-centered inflammation and lipid alterations. *J Allergy Clin Immunol* 2018;141:2094–106.
- Caubet C, Jonca N, Brattsand M, Guerrin M, Bernard D, Schmidt R, et al. Degradation of corneodesmosome proteins by two serine proteases of the kallikrein family, SCTE/KLK5/hK5 and SCCE/KLK7/hK7. *J Invest Dermatol* 2004;122:1235–44.
- Chavanas S, Bodemer C, Rochat A, Hamel-Teillac D, Ali M, Irvine AD, et al. Mutations in SPINK5, encoding a serine protease inhibitor, cause netherton syndrome. *Nat Genet* 2000;25:141–2.
- Czarnowicki T, He H, Krueger JG, Guttman-Yassky E. Atopic dermatitis endotypes and implications for targeted therapeutics. *J Allergy Clin Immunol* 2019;143:1–11.
- DaVeiga SP. Epidemiology of atopic dermatitis: a review. *Allergy Asthma Proc* 2012;33:227–34.
- Deraison C, Bonnart C, Lopez F, Besson C, Robinson R, Jayakumar A, et al. LEKTI Fragments Specifically Inhibit KLK5, KLK7, and KLK14 and Control Desquamation through a pH-dependent Interaction. *Mol Biol Cell* 2007;18:3607–19.
- Descargues P, Deraison C, Bonnart C, Kreft M, Kishibe M, Ishida-Yamamoto A, et al. Spink5-deficient mice mimic netherton syndrome through degradation of desmoglein 1 by epidermal protease hyperactivity. *Nat Genet* 2005;37:56–65.
- Dobin A, Davis CA, Schlesinger F, Drenkow J, Zaleski C, Jha S, et al. STAR: ultrafast universal RNA-seq aligner. *Bioinformatics* 2013;29:15–21.
- Drucker AM, Wang AR, Li WQ, Severson E, Block JK, Qureshi AA. The burden of atopic dermatitis: summary of a report for the National Eczema Association. *J Invest Dermatol* 2017;137:26–30.
- Eichenfield LF, Tom WL, Chamlin SL, Feldman SR, Hanifin JM, Simpson EL, et al. Guidelines of care for the management of atopic dermatitis: section 1. Diagnosis and assessment of atopic dermatitis. *J Am Acad Dermatol* 2014;70:338–51.

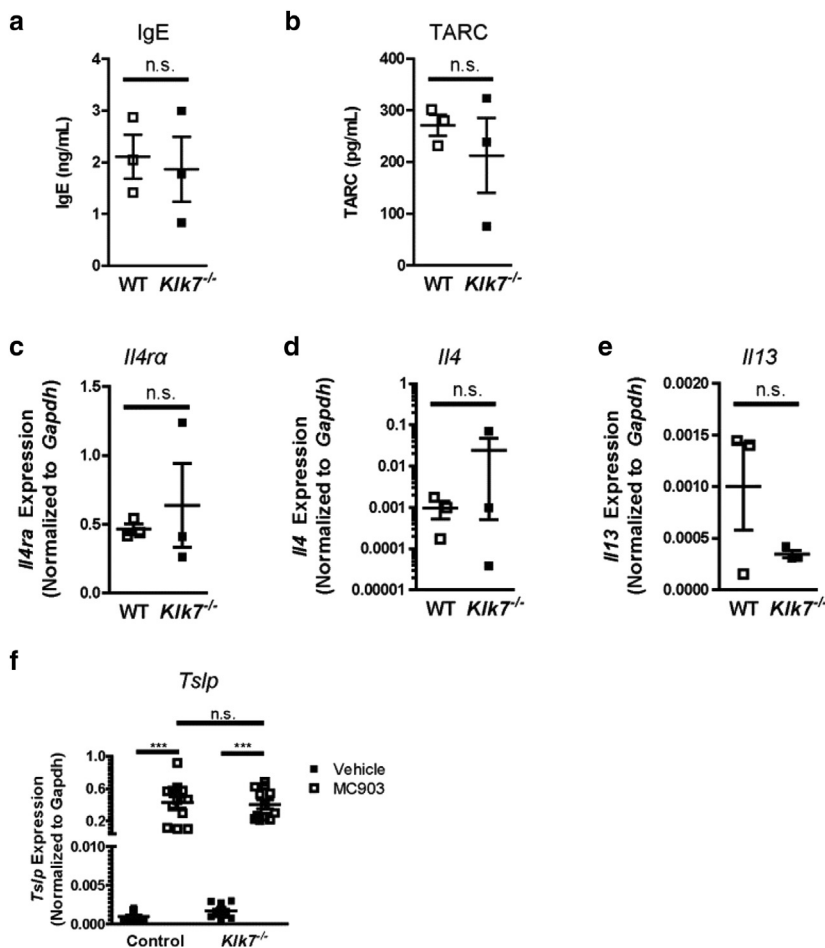
- Ekhholm IE, Brattsand M, Egelrud T. Stratum corneum tryptic enzyme in normal epidermis: a missing link in the desquamation process? *J Invest Dermatol* 2000;114:56–63.
- Elias PM, Hatano Y, Williams ML. Basis for the barrier abnormality in atopic dermatitis: outside-inside-outside pathogenic mechanisms. *J Allergy Clin Immunol* 2008;121:1337–43.
- Esaki H, Ewald DA, Ungar B, Rozenblit M, Zheng X, Xu H, et al. Identification of novel immune and barrier genes in atopic dermatitis by means of laser capture microdissection. *J Allergy Clin Immunol* 2015;135:153–63.
- Fagerberg L, Hallström BM, Oksvold P, Kampf C, Djureinovic D, Odeberg J, et al. Analysis of the human tissue-specific expression by genome-wide integration of transcriptomics and antibody-based proteomics. *Mol Cell Proteomics* 2014;13:397–406.
- Furio L, de Veer S, Jaillat M, Briot A, Robin A, Deraison C, et al. Transgenic kallikrein 5 mice reproduce major cutaneous and systemic hallmarks of netherton syndrome. *J Exp Med* 2014;211:499–513.
- Gao YJ, Ji RR. c-Fos and pERK, which is a Better Marker for Neuronal Activation and Central Sensitization after Noxious Stimulation and Tissue Injury? *Open Pain J* 2009;2:11–7.
- Guttman-Yassky E, Bissonnette R, Ungar B, Suárez-Fariñas M, Ardeleanu M, Esaki H, et al. Dupilumab progressively improves systemic and cutaneous abnormalities in patients with atopic dermatitis. *J Allergy Clin Immunol* 2019;143:155–72.
- Han L, Ma C, Liu Q, Weng HJ, Cui Y, Tang Z, et al. A subpopulation of nociceptors specifically linked to itch. *Nat Neurosci* 2013;16:174–82.
- Hansson L, Bäckman A, Ny A, Edlund M, Ekhholm E, Hammarström BE, et al. Epidermal overexpression of stratum corneum chymotryptic enzyme in mice: A model for chronic itchy dermatitis. *J Invest Dermatol* 2002;118:444–9.
- Howell MD, Kim BE, Gao P, Grant AV, Boguniewicz M, DeBenedetto A, et al. Cytokine modulation of atopic dermatitis filaggrin skin expression. *J Allergy Clin Immunol* 2007;120:150–5.
- Huang CC, Yang W, Guo C, Jiang H, Li F, Xiao M, et al. Anatomical and functional dichotomy of ocular itch and pain. *Nat Med* 2018;24:1268–76.
- Kasperek P, Ileninova Z, Zbodakova O, Kanchev I, Benada O, Chalupsky K, et al. KLK5 and KLK7 ablation fully rescues lethality of netherton syndrome-like phenotype. *PLOS Genet* 2017;13:e1006566.
- Kaufman BP, Guttman-Yassky E, Alexis AF. Atopic dermatitis in diverse racial and ethnic groups—variations in epidemiology, genetics, clinical presentation and treatment. *Exp Dermatol* 2018;27:340–57.
- Kim BS. Innate lymphoid cells in the skin. *J Invest Dermatol* 2015;135:673–8.
- Kim BS, Siracusa MC, Saenz SA, Noti M, Monticelli LA, Sonnenberg GF, et al. TSLP elicits IL-33-independent innate lymphoid cell responses to promote skin inflammation. *Sci Transl Med* 2013;5:170ra16.
- Kim BS, Wang K, Siracusa MC, Saenz SA, Brestoff JR, Monticelli LA, et al. Basophils promote innate lymphoid cell responses in inflamed skin. *J Immunol* 2014;193:3717–25.
- Komatsu N, Saijoh K, Kuk C, Liu AC, Khan S, Shirasaki F, et al. Human tissue kallikrein expression in the stratum corneum and serum of atopic dermatitis patients. *Exp Dermatol* 2007;16:513–9.
- Komatsu N, Saijoh K, Toyama T, Ohka R, Otsuki N, Hussack G, et al. Multiple tissue kallikrein mRNA and protein expression in normal skin and skin diseases. *Br J Dermatol* 2005;153:274–81.
- Komatsu N, Takata M, Otsuki N, Toyama T, Ohka R, Takehara K, et al. Expression and localization of tissue kallikrein mRNAs in human epidermis and appendages. *J Invest Dermatol* 2003;121:542–9.
- Leung DYM. Atopic dermatitis: age and race do matter! *J Allergy Clin Immunol* 2015;136:1265–7.
- Li M, Hener P, Zhang Z, Kato S, Metzger D, Chambon P. Topical vitamin D3 and low-calcemic analogs induce thymic stromal lymphopoietin in mouse keratinocytes and trigger an atopic dermatitis. *Proc Natl Acad Sci USA* 2006;103:11736–41.
- Liao Y, Smyth GK, Shi W. featureCounts: an efficient general purpose program for assigning sequence reads to genomic features. *Bioinformatics* 2014;30:923–30.
- Liu Q, Weng HJ, Patel KN, Tang Z, Bai H, Steinhoff M, et al. The distinct roles of two GPCRs, MrgprC11 and PAR2, in itch and hyperalgesia. *Sci Signal* 2011;4:ra45.
- Love MI, Huber W, Anders S. Moderated estimation of fold change and dispersion for RNA-seq data with DESeq2. *Genome Biol* 2014;15:550.
- Margolis DJ, Gupta J, Apter AJ, Ganguly T, Hoffstad O, Papadopoulos M, et al. Filaggrin-2 variation is associated with more persistent atopic dermatitis in African American subjects. *J Allergy Clin Immunol* 2014;133:784–9.
- Mashiko S, Mehta H, Bissonnette R, Sarfati M. Increased frequencies of basophils, type 2 innate lymphoid cells and Th2 cells in skin of patients with atopic dermatitis but not psoriasis. *J Dermatol Sci* 2017;88:167–74.
- Morizane S, Yamasaki K, Kajita A, Ikeda K, Zhan M, Aoyama Y, et al. TH2 cytokines increase kallikrein 7 expression and function in patients with atopic dermatitis. *J Allergy Clin Immunol* 2012;130:259–61.e1.
- Nattkemper LA, Tey HL, Valdes-Rodriguez R, Lee H, Mollanazar NK, Albornoz C, et al. The genetics of chronic itch: gene expression in the skin of patients with atopic dermatitis and psoriasis with severe itch. *J Invest Dermatol* 2018;138:1311–7.
- Oetjen LK, Kim BS. Interactions of the immune and sensory nervous systems in atopy. *FEBS Journal* 2018;285:3138–51.
- Oetjen LK, Mack MR, Feng J, Whelan TM, Niu H, Guo CJ, et al. Sensory Neurons Co-opt Classical Immune Signaling Pathways to Mediate Chronic Itch. *Cell* 2017;171:217–28.e13.
- Osawa R, Akiyama M, Shimizu H. Filaggrin gene defects and the risk of developing allergic disorders. *Allergol Int* 2011;60:1–9.
- Palmer CNA, Irvine AD, Terron-Kwiatkowski A, Zhao Y, Liao H, Lee SP, et al. Common loss-of-function variants of the epidermal barrier protein filaggrin are a major predisposing factor for atopic dermatitis. *Nat Genet* 2006;38:441–6.
- Pavlopoulou A, Pampalakis G, Michalopoulos I, Sotiropoulou G. Evolutionary history of tissue kallikreins. *PLOS ONE* 2010;5:e13781.
- Shaw JLV, Diamandis EP. Distribution of 15 human kallikreins in tissues and biological fluids. *Clin Chem* 2007;53:1423–32.
- Shimada SG, Shimada KA, Collins JG. Scratching behavior in mice induced by the proteinase-activated receptor-2 agonist, SLIGRL-NH2. *Eur J Pharmacol* 2006;530:281–3.
- Silverberg JL. Public health burden and epidemiology of atopic dermatitis. *Dermatol Clin* 2017;35:283–9.
- Simpson EL, Bieber T, Guttman-Yassky E, Beck LA, Blauvelt A, Cork MJ, et al. Two phase 3 Trials of Dupilumab versus Placebo in Atopic Dermatitis. *N Engl J Med* 2016;375:2335–48.
- Sotiropoulou G, Pampalakis G, Diamandis EP. Functional roles of human Kallikrein-related peptidases. *J Biol Chem* 2009;284:32989–94.
- Stefansson K, Brattsand M, Roosterman D, Kempkes C, Bocheva G, Steinhoff M, et al. Activation of proteinase-activated receptor-2 by human kallikrein-related peptidases. *J Invest Dermatol* 2008;128:18–25.
- Thaçi D, Simpson EL, Beck LA, Bieber T, Blauvelt A, Papp K, et al. Efficacy and safety of dupilumab in adults with moderate-to-severe atopic dermatitis inadequately controlled by topical treatments: A randomised, placebo-controlled, dose-ranging phase 2b trial. *Lancet* 2016;387:40–52.
- Trier AM, Kim BS. Cytokine modulation of atopic itch. *Curr Opin Immunol* 2018;54:7–12.
- Vasilopoulos Y, Sharaf N, di Giovine F, Simon M, Cork MJ, Duff GW, et al. The 3'-UTR AACCins5874 in the stratum corneum chymotryptic enzyme gene (SCCE/CLK7), associated with atopic dermatitis; causes an increased mRNA expression without altering its stability. *J Dermatol Sci* 2011;61:131–3.
- Yousef GM, Scorilas A, Magklara A, Soosapillai A, Diamandis EP. The KLK7 (PRSS6) gene, encoding for the stratum corneum chymotryptic enzyme is a new member of the human kallikrein gene family - Genomic characterization, mapping, tissue expression and hormonal regulation. *Gene* 2000;254:119–28.



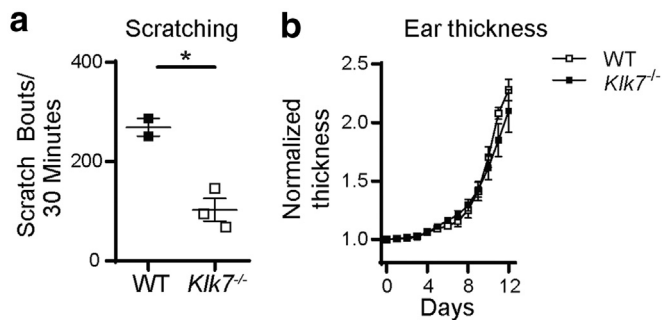
Supplementary Figure S1. *KLK7*, but not *KLK5*, is upregulated in human lesional AD skin. (a) Log₂ read CPM of *KLK5* in control skin from donors without AD (N = 20, age = 36.8 ± 2.4 years, 42.9% female), and matched pairs of NL skin and LS from donors with AD (N = 35, age = 34.3 ± 2.5 years, 50% female). (b) Log₂ CPM of *KLK7* in the same RNA-Seq data set. Note that *KLK7* is overexpressed only in LS from donors with AD. * $P < 0.05$. ** $P < 0.01$. (c) Pearson correlation between *KLK7* transcript abundance in lesional skin and the VAS itch scores from patients with AD. $R = 0.22$ (CI = -0.13 to 0.52), $P = 0.22$. Error bars = standard error of the mean. AD, atopic dermatitis; CPM, counts per million; LS, lesional skin; NL, nonlesional; n.s., no significance; RNA-Seq, RNA Sequencing; VAS, visual analog scale.



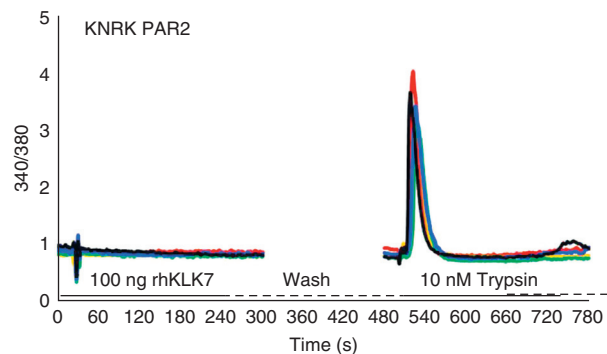
Supplementary Figure S2. *Kik7* expression is restricted to the epidermis in mouse skin. (a) Genomic construct of the *Kik7^{tm1(KOMP)Vlcg}* allele. Exons 3-5 within the coding region of *Kik7* are replaced with a *LacZ*- β -galactosidase reporter. (b) X-gal staining (blue) of hair-bearing skin from a *Kik7^{LacZ}* mouse, in which *LacZ* expression is controlled under the *Kik7* promoter. (c–f) X-gal staining of (c) DRG, (d) TG, (e) SC, (f) and brain. (g) RT-PCR screening of *Kik7* expression in tissues from a WT control mouse. N = 3 biological replicates for panels (b–g). Scale bars = 200 μ m. Cere., cerebrum; Cebel., cerebellum; DRG, dorsal root ganglia; Epidid., epididymis; Esoph., esophagus; G skin, glabrous skin; H skin, hairy skin; *LacZ*, β -galactosidase; RT-PCR, reverse transcriptase–PCR; SC, spinal cord; SI, Small intestine; TG, trigeminal ganglia; WT, wild-type.



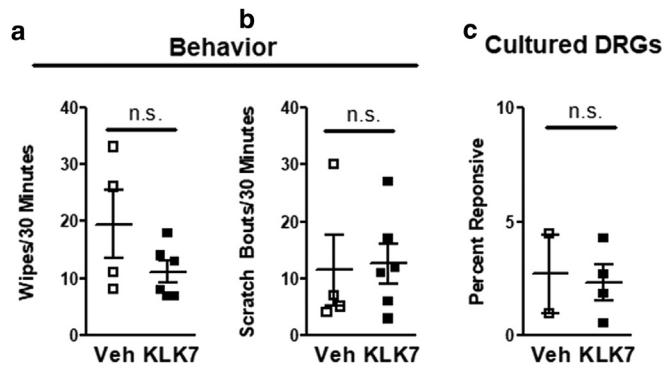
Supplementary Figure S3. *Kik7*^{-/-} mice do not show lowered Th2 and inflammatory markers after MC903 Treatment. (a, b) ELISA-based quantification of serum (a) IgE and (b) TARC levels in MC903-treated control and *Kik7*^{-/-} mice. (c–e) RT-qPCR quantification of (c) *Il4ra*, (d) *Il4*, and (e) *Il13* expression in MC903-treated skin of control and *Kik7*^{-/-} mice. (f) RT-qPCR quantification of *Tslp* expression in vehicle or MC903-treated skin of control and *Kik7*^{-/-} mice. Error bars = standard error of the mean. ****P* < 0.001. MC903, calcipotriol; n.s., no significance, RT-qPCR, quantitative reverse transcriptase–PCR; TARC, thymus and activation-regulated chemokine.



Supplementary Figure S4. *Kik7*^{-/-} mice have a selective reduction in itch in MC903 ear model. (a) Scratching behavior recorded on day 12 of MC903 treatment of control (wild-type) and *Kik7*^{-/-} mice. (b) Change in ear thickness (normalized to pretreatment baseline) as measured by calipers daily during topical MC903 treatment. Error bars = standard error of the mean. ***P* < 0.05. WT, wild-type.



Supplementary Figure S5. rhKLK7 does not activate PAR2 receptors. Representative calcium transients of KNRK cells stably transfected with PAR2 expression after treatment with rhKLK7 and trypsin.



Supplementary Figure S6. Acute *in vivo* and *in vitro* effects of rhKLK7. (a, b). Acute pain (wiping) and itch (scratching) behavioral responses of C57BL/6J mice to vehicle or 1 μg rhKLK7 injections. (c) Quantification of calcium responses of culture DRG neurons from *Pir1^{GCaMP3/+}* mice to acute application of vehicle or 20 ng/μl rhKLK7. Percent responsive represents fraction of all DRG neurons in field. Data is presented as mean ± standard error of the mean. DRG, dorsal root ganglia; n.s, no significance.

Supplementary Table S1. Primers used for PCR

Gene	Forward Primer	Reverse Primer
<i>HS KLK5</i>	CACAAGGGTAATCTCCCCAG	AGATGACACCATGTTCTGCG
<i>HS KLK7</i>	GGGTACCTCTGCACCAAC	GGATGTCAAGTCATCTCCC
<i>HS ACTB</i>	ACCTTCTACAATGAGCTGCG	CCTGGATAGCAACGTACATGG
<i>MM Klk5</i>	GAACCACTTAGCCTCGACCTTTAT	GTTCCGGTTCAGAGGGGTTG
<i>MM Klk7</i>	GTGCTGGCATTCTGACTCTA	CCATCACCCACCGTTTGTACT
<i>MM Gapdh</i>	CCCAGCAAGGACACTGAGCAA	TATGGGGGTCTGGGATGGAAA
<i>MM Il4α</i>	GTTACAGGAACAAGACCAGCA	TGGAGCCTGAACTCGCA
<i>MM Il4</i>	GAACGAGGTACAGGAGAAG	ACCTTGGAAAGCCCTACAGA
<i>MM Il13</i>	TGCCATCTACAGGCCAGCA	CTCATTAGAAGGGGCCGTGG

Supplementary Table S2. Primary Antibodies for Flow Cytometry

Antibody	Vendor	Catalog #	Antibody	Vendor	Catalog #
CD49b APC	Biologend	17-5971-82	Siglec-F BV421	BD	562681
CD11b BV510	Biologend	101245	CD117 BV605	Biologend	135122
CD3ε PerCP/Cy5.5	eBioscience	45-0031-82	CD5 PerCP/Cy5.5	eBioscience	45-0051-82
CD11c PerCP/Cy5.5	eBioscience	45-0114-82	CD19 PerCP/Cy5.5	eBioscience	45-0193-82
NK1.1 PerCP/Cy5.5	eBioscience	45-5941-82	ST2-Biotin	Biologend	145307
KLRG1 PE/Dazzle	Biologend	138424	CD25 BV605	Biologend	102035
FcεRIα FITC	eBioscience	11-5898-85	IgE FITC	eBioscience	11-5992-81
CD90.2 PE/Cy7	Biologend	140309	CD45 APC	Biologend	103111
CD45.2 PE	Biologend	109808	CD3ε PE	Biologend	100307